Dalton Transactions

RSC Publishing

PAPER

View Article Online
View Journal | View Issue

Cite this: *Dalton Trans.*, 2013, **42**, 11005

Improved luminescence and temperature sensing performance of Ho^{3+}–Yb^{3+}–Zn^{2+}:Y_2O_3 phosphor

Anurag Pandey and Vineet Kumar Rai*

Received 4th March 2013,
Accepted 9th May 2013

DOI: 10.1039/c3dt50592h

www.rsc.org/dalton

The codoping effect of Zn^{2+} ions on luminescence emission in visible and near infrared (NIR) regions of Y_2O_3:Ho^{3+}–Yb^{3+} phosphor prepared by low temperature combustion process have been investigated under 980 nm and 448 nm excitations. The phase and crystallite size of the prepared phosphor were determined by X-ray diffraction analysis and processes involved in the upconversion mechanism have been discussed in detail *via* pump power dependence, decay curve analysis and a suitable energy level diagram. The temperature sensing performance of the developed material has also been investigated by measuring the fluorescence intensity ratio of the blue upconversion emission bands centred at 465 nm and 491 nm up to 673 K. It is found that by using fluorescence intensity ratio technique, appreciable sensitivity for temperature measurement can be achieved from the present phosphor material, which indicates its applicability as a high temperature sensing probe. The fabrication of green LEDs using the developed phosphor material has also been suggested.

1. Introduction

Rare earth doped phosphors have been extensively used in solid state lighting, display devices, light emitting diodes, enhancement of solar cell efficiency, biological and therapeutic application, development of laser and temperature sensing devices *etc.*[1–7] The investigation of new and efficient luminescence materials are of great attraction among researchers nowadays. The development and improvement of phosphor materials still continues due to its increased demand over glassy and other materials. The luminescence emission from lanthanide doped phosphors has been modified by codoping with other lanthanides and transition metals. Mostly the incorporation of ytterbium ions into different rare earth doped solid hosts have been investigated for this purpose.[8–15] Furthermore, investigations on bismuth,[16] lithium,[17–20] calcium, barium, strontium,[21,22] aluminium, magnesium,[23] zinc,[24–26] silver,[27] gold[28] and manganese[29] codoped phosphors have also been carried out for improving the luminescence efficiency.

Liu *et al.*[16] studied the codoping effect of Bi^{3+} into Sm^{3+} doped Gd_2O_3 phosphor and found about 8-fold emission intensity enhancement on Bi^{3+} codoping. The effect of the addition of lithium ions on the photoluminescence intensity of the rare earth ions doped into various solid host materials have been studied by different researchers.[17–20] Hyeon *et al.*[22] studied the enhancement in photoluminescence (PL) intensity of $SrTiO_3$:Pr phosphor by substitution of (Li, La) pair for strontium. The enhancement of the red emission intensity in the Y_2O_3:Eu^{3+} phosphor due to the incorporation of the Mg^{2+}/Al^{3+} ions has been studied by Chong *et al.*[23] The enhancement by about 37 times in the green emission intensity of Nd^{3+} ions doped in the Y_2O_3 phosphor due to presence of Zn^{2+} ions upon excitation at 980 nm has also been observed.[24] Singh *et al.*[26] studied the effect of Zn^{2+} incorporation in the Al_2O_3:Er^{3+}–Yb^{3+} phosphor and found enhancement by about 7 times and 34 times in green and red regions, respectively. The selective enhancement of green UC emission in the Er^{3+}:$Yb_3Al_5O_{12}$ nanocrystals followed by the energy transfer from the highly excited state Yb^{3+}–Mn^{2+} dimer has been monitored.[29] These investigations show that the codoping of rare earth and/or non rare earths into different lanthanide doped phosphor materials improve the luminescence property of material.

Several discussions and investigations on tridoped luminescence materials have been reported[20,24,26,29–33] but no such study on Ho^{3+}–Yb^{3+}–Zn^{2+} codoped materials has been found to the best of our knowledge. Gutzov *et al.*[33] reported high temperature optical spectroscopy of $Zr_{0.78}Y_{0.18}Sm_{0.04}O_{1.89}$ and $Zr_{0.78}Y_{0.18}Ho_{0.04}O_{1.89}$ single crystals up to 1323 K and concluded that the prepared material can be used in making high temperature UV-filters. Among the oxide host materials, yttrium oxide is of particular interest here as a host for its special characteristics and suitable matching of ionic radii with many rare earth ions.[34] Combustion route is taken as synthesis procedure due to its advantage over other conventional preparation techniques.[24] Solution combustion method gives

Laser and Spectroscopy Laboratory, Department of Applied Physics, Indian School of Mines, Dhanbad-826004, Jharkhand, India. E-mail: vineetkrrai@yahoo.co.in, rai.vk.ap@ismdhanbad.ac.in; Tel: +91-326-223 5404/5282

direct crystallization of smaller-sized particles utilizing a low processing temperature in a short time compared to solid state synthesis and gives uniform doping of impurity ions.

Recently, sensors based on monitoring the temperature by using the fluorescence intensity ratio (FIR) technique have been used as optical temperature sensors, playing a vital role in the places where conventional sensors can not be used. For any optical temperature sensor, the operating temperature range and the emission efficiency should be high. The search for such materials is still challenging.

In this paper, we report the effect of Zn^{2+} codoping into Y_2O_3:Ho^{3+}–Yb^{3+} phosphor prepared by combustion synthesis technique upon 980 nm and 448 nm excitations. The phenomenon involved in the emission process has been confirmed by pump power dependence, decay curve analysis and an energy level diagram. The temperature sensing behaviour in the developed phosphor has been investigated using fluorescence intensity ratio technique of two close lying levels, responsible for the blue upconversion emission of holmium ions.

2. Experimental

2.1 Sample preparation by combustion technique

The Ho^{3+}, Yb^{3+}, Zn^{2+} codoped Y_2O_3 phosphors were synthesized by solution combustion method.[35] The starting materials were Y_2O_3, Ho_2O_3, Yb_2O_3 and ZnO, while urea was used as the organic fuel. The composition of compound used was the following:

$$(100 - x - y - z)Y_2O_3 + xHo_2O_3 + yYb_2O_3 + zZnO \qquad \text{(i)}$$

where x = 0.2 mol%, y = 3 mol% and z = 0, 5, 10, 15, 20, 25 mol%.

The desired amounts of starting materials were first dissolved in nitric acid (HNO_3) to obtain a transparent solution. The transparent solution was then mixed with urea in 1 : 2 proportion (molar %). The solution was heated at 60 °C and stirred at 1000 rpm with the help of a magnetic stirrer, for nearly two hours to form a transparent gel. The transparent gel was then rapidly heated in a furnace preheated at 600 °C. In 2 to 5 minutes, the solution became foamed and a flame was produced that lasted a few minutes. The sample was immediately removed from the furnace. The resultant fluffy mass was then taken out and crushed into fine powder using a pestle and mortar. The formed Y_2O_3:Ho^{3+}–Yb^{3+} and Y_2O_3:Ho^{3+}–Yb^{3+}–Zn^{2+} phosphor powders were annealed at 800 °C and then used for further optical characterization purposes.

2.2 Characterization of prepared samples

The X-ray powder diffraction pattern of developed phosphors were recorded by an X-ray diffractometer using Cu $K\alpha_1$ radiation (λ = 0.154 nm) in the 10 to 80° range. The UC emission spectra were recorded using a Princeton triple turret grating monochromator (Acton SP-2300) attached to a photomultiplier tube (PMT) and personal computer (PC). The samples were irradiated by a diode (CW) laser operating at 980 nm of spot size 1.4 mm with different powers. The fluorescence studies were carried out using a fluorescence spectrophotometer. The lifetime analysis experiments were performed by chopping the 980 nm laser beam by a mechanical chopper and measurements were made with the help of quick start digital oscilloscope. For the temperature measurements, the sample was placed in a small homemade furnace and heated from room temperature to 673 K, measured with the help of a thermocouple located closer to the sample.

3. Results and discussion

3.1 X-ray diffraction analysis

The X-ray diffraction patterns of the Ho^{3+}–Yb^{3+} and Ho^{3+}–Yb^{3+}–Zn^{2+} codoped Y_2O_3 phosphors heat treated at 800 °C are shown in Fig. 1(a). The main peaks are indexed and match with cubic phase pure Y_2O_3 (JCPDS file no. 25-1200). It was concluded that the samples are well crystalline and no

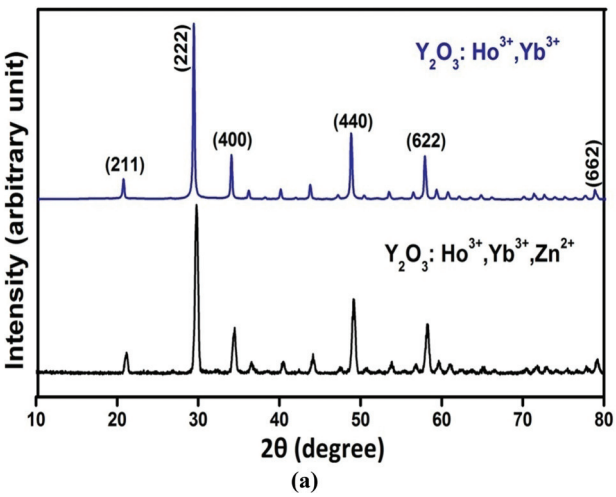

(a)

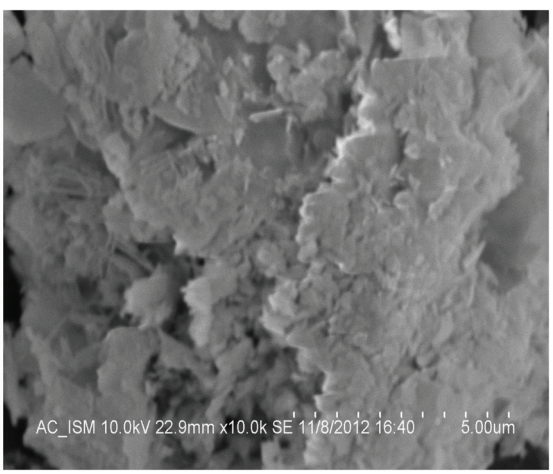

(b)

Fig. 1 (a) X-ray diffraction pattern of Y_2O_3:Ho^{3+}–Yb^{3+} and Y_2O_3:Ho^{3+}–Yb^{3+}–Zn^{2+} phosphors. (b) SEM micrograph of Y_2O_3:Ho^{3+}–Yb^{3+}–Zn^{2+} phosphor powder heat treated at 800 °C.

additional peaks were detected upon Zn^{2+} codoping, although a slight shift is observed towards higher 2θ value. This shift happens due to slight retrenchment of the unit cell volume[36] caused by difference in ionic radii of Y^{3+} (~90 pm) and Zn^{2+} (~74 pm) ions. Also, the average crystallite size of the phosphors calculated by Scherrer's formula[37] using the assigned peaks is found to decrease upon codoping with the Zn^{2+} ions. The average crystallite size in the Ho^{3+}–Yb^{3+} and Ho^{3+}–Yb^{3+}–Zn^{2+} codoped Y_2O_3 phosphors are around 43 nm and 22 nm, respectively. The nano sized crystalline nature of Ho^{3+} doped Y_2O_3 phosphor by using transmission electron microscopy (TEM) has also been reported.[38]

3.2 Scanning electron microscopy (SEM)

To determine surface morphology of the prepared sample, SEM image of Y_2O_3:Ho^{3+}–Yb^{3+}–Zn^{2+} phosphor heat treated at 800 °C was recorded and is shown in Fig. 1(b). From the figure it is clear that particles are in agglomerated form with size in the micrometer range. The SEM image also shows the inhomogeneous distribution of the particles due to the non-uniform distribution of temperature and mass flow in the combustion flame during the combustion process.

3.3 Luminescence studies

To investigate the UC emission property of Y_2O_3:Ho^{3+}–Yb^{3+}–Zn^{2+} phosphor, a series of samples were prepared on varying the concentration of Zn^{2+} with optimized 0.2 mol% of Ho^{3+} and 3 mol% of Yb^{3+} concentrations.[39] The variation in UC emission intensity *versus* Zn^{2+} concentration upon 980 nm excitation is shown in the inset of Fig. 2. The upconversion emission intensity varies with the increase in the Zn^{2+} ion concentration and is observed to be maximised at 10 mol% Zn^{2+} ions. All further measurements were done using this concentration. Fig. 2 shows the room temperature UC emission spectra of as-synthesized 0.2 mol% Ho^{3+} + 3 mol% Yb^{3+} and 0.2 mol% Ho^{3+} + 3 mol% Yb^{3+} + 10 mol% Zn^{2+} codoped Y_2O_3 phosphors upon 980 nm (CW) diode laser excitation in 450–800 nm wavelength range.

The observed UC emission bands centred at 465, 491, 546, 658 and 757 nm have been assigned to the $^3K_8 \rightarrow {}^5I_8$, $^5F_3 \rightarrow {}^5I_8$, $^5F_4/{}^5S_2 \rightarrow {}^5I_8$, $^5F_5 \rightarrow {}^5I_8$ and $^5S_2 \rightarrow {}^5I_7$ transitions of the holmium ion, respectively.[39,40] The addition of Zn^{2+} to the Y_2O_3:Ho^{3+}–Yb^{3+} phosphor enhanced the UC emission intensities by ~11 times, ~7 times, ~3 times and ~7 times in the blue, green, red and NIR bands, respectively. This significant enhancement in UC emission intensity is due to presence of the local field around the Ho^{3+} ions followed by the substitutional effect. The larger ionic radii of Y^{3+} ion (~90 pm) compared to Zn^{2+} ion (~74 pm) causes the substitution of Y^{3+} ions by the Zn^{2+} ions and hence induces the contraction in the host lattice. Due to the substitutional effect the local crystal field symmetry around the rare earth ion (Ho^{3+}) is modified. The fluorescence decay curve for $^5S_2 \rightarrow {}^5I_8$ transition of holmium ions in both the phosphors were monitored (shown in Fig. 3). The lifetimes observed from the decay curve analysis are 1380.0 ± 18.9 μs and 967.5 ± 8.4 μs in the case of Y_2O_3:Ho^{3+}–Yb^{3+} and Y_2O_3:Ho^{3+}–Yb^{3+}–Zn^{2+} phosphors, respectively. This observed variation in decay time of emitting level is attributed to the local field effect arises due to codoping of Zn^{2+} ions.[41] The decrease in decay time increases the transition probability of emitting states and hence the radiative emissions.

Moreover, the green to red ratio of Y_2O_3:Ho^{3+}–Yb^{3+} phosphor increased from 14.52 to 34.03 upon codoping with Zn^{2+} ions, which improved the purity of the green colour emitted from the sample. The variation in colour emitted from samples can be visualised by the CIE chromaticity diagram (Fig. 4). From this figure, we observed that the colour coordinate shift towards the pure green region in the case of Zn^{2+} codoped phosphor indicating an improvement in the purity of green colour emitted from synthesized phosphor. Also, the pump power increment of the Y_2O_3:Ho^{3+}–Yb^{3+}–Zn^{2+} phosphor shows enhancement in UC emission intensity for all observed bands (Fig. 5). It is remarkable to note that the values of colour coordinates at different pump powers are

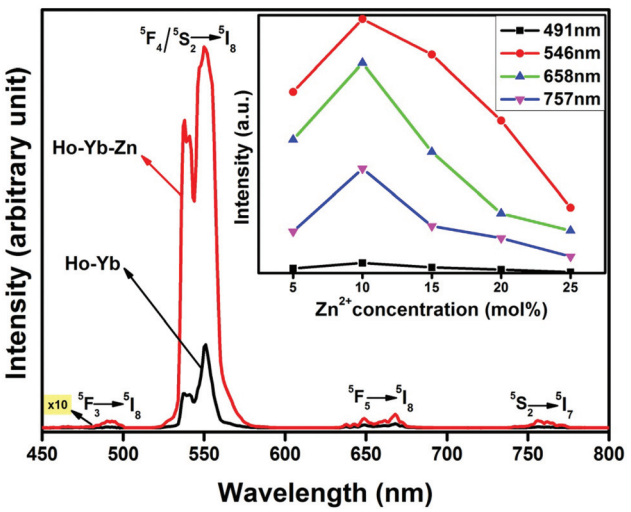

Fig. 2 Upconversion emission spectra of Y_2O_3:Ho^{3+}–Yb^{3+} and Y_2O_3:Ho^{3+}–Yb^{3+}–Zn^{2+} phosphors along with concentration dependence of Zn^{2+} ions.

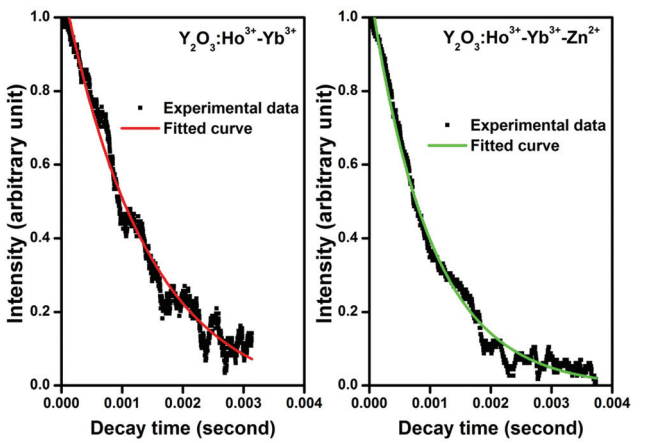

Fig. 3 Luminescence decay curve for $^5S_2 \rightarrow {}^5I_8$ transition of Y_2O_3:Ho^{3+}–Yb^{3+} and Y_2O_3:Ho^{3+}–Yb^{3+}–Zn^{2+} phosphors.

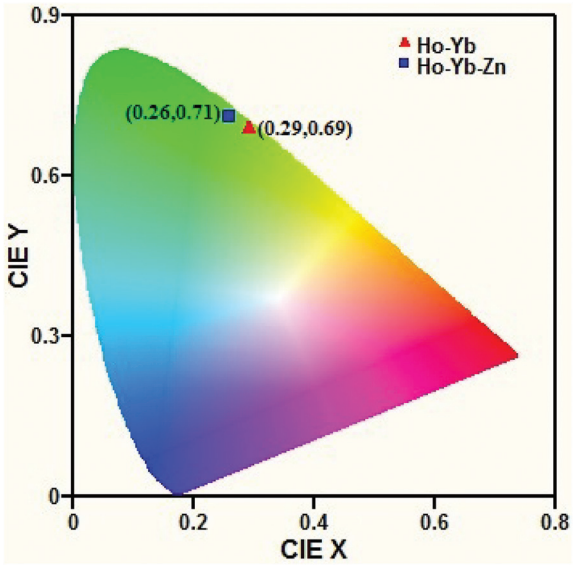

Fig. 4 CIE colour coordinates of Y_2O_3:Ho^{3+}–Yb^{3+} and Y_2O_3:Ho^{3+}–Yb^{3+}–Zn^{2+} phosphors.

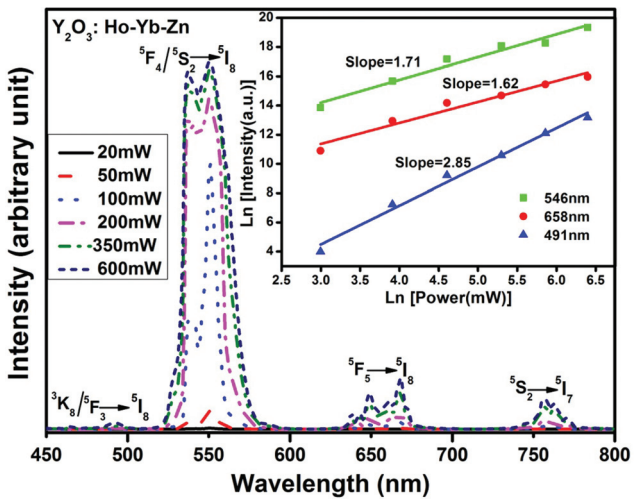

Fig. 5 Upconversion emission spectra at different powers and logarithmic dependence of peak intensity of blue, green and red UC emissions as a function of pump power for Y_2O_3:Ho^{3+}–Yb^{3+}–Zn^{2+} phosphor.

almost the same, indicating no colour tunability in the present phosphor. This high purity intense green emitting phosphor can be used in the development of display devices.[42] Additionally, the green light coming from the present sample having a small power density of 0.004 to 1.015 W cm^{-2} at pump excitation powers of 5 to 1560 mW may trigger the selective photochemical reaction that occurs in photodynamic therapy (PDT).[35,43] It was also reported that rare earth doped upconverting materials are very suitable for biological applications such as bioconjugation and bioimaging due to their negligible autofluorescence.[1] Actually, the NIR excitations (used to excite upconverting materials) have great advantages in cell and tissue imaging owing to the following reasons: strong penetration ability *i.e.* penetrates deeper into tissues; less photo damage *i.e.* after irradiation for a long time, the tissues remains safe; and high signal to noise ratio.[44] As the Y_2O_3:Ho^{3+}–Yb^{3+}–Zn^{2+} phosphor emits intense green light upon 980 nm excitation, it may be the subject of study as an alternative of traditional fluorescent biolabels for *in vitro* cell imaging and *in vivo* tissue imaging in the future.

It is well known that the intensity of UC emission (I) is directly proportional to the kth power of pump power (P)[35] as

$$I \propto P^k \quad \text{(ii)}$$

where k is the number of pump photons required to populate the emission bands. The variation of logarithmic of pump power as a function of UC emission intensity for blue, green and red bands centred at 491 nm, 546 nm and 658 nm, respectively is shown in inset of Fig. 5. The slopes obtained from the figure decided the number of pump photons and was found to be three for the blue band and two for the other bands.

Fig. 6 shows the energy level diagram of the Ho^{3+} and Yb^{3+} ions with a possible transition scheme. The $^5I_6$ state of Ho^{3+} ion is populated through ground state absorption (GSA) of a 980 nm photon as well as by energy transfer (ET) from Yb^{3+} to Ho^{3+} ions. The excited ions in $^5I_6$ state are again promoted to the $^5F_4/^5S_2$ level *via* excited state absorption and efficient energy transfer process. The populated $^5F_4/^5S_2$ level relaxes radiatively to ground states $^5I_8$ and $^5I_7$ and emits intense green and NIR emission around 546 nm and 757 nm, respectively. A part of population in these states can also relax to the $^5F_5$ level *via* multiphonon relaxation and from there *via* radiative relaxation to ground state gives red emission at about 658 nm. Furthermore, the upper levels are also populated by three photon absorption processes and give emissions around 465 nm and 491 nm through $^3K_8 \rightarrow {}^5I_8$ and $^5F_3 \rightarrow {}^5I_8$ transitions, respectively, as explained in our previous report.[39]

Fig. 7(a) shows the excitation spectra of Y_2O_3:Ho^{3+}–Yb^{3+} and Y_2O_3:Ho^{3+}–Yb^{3+}–Zn^{2+} phosphors keeping emission lines fixed at 546 nm ($^5F_4/^5S_2 \rightarrow {}^5I_8$). The excitation bands were

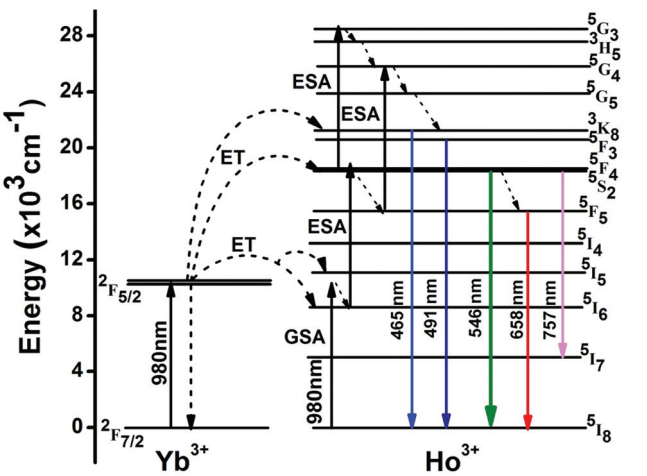

Fig. 6 Energy level diagram of the Ho^{3+} and Yb^{3+} ions with possible transition scheme.

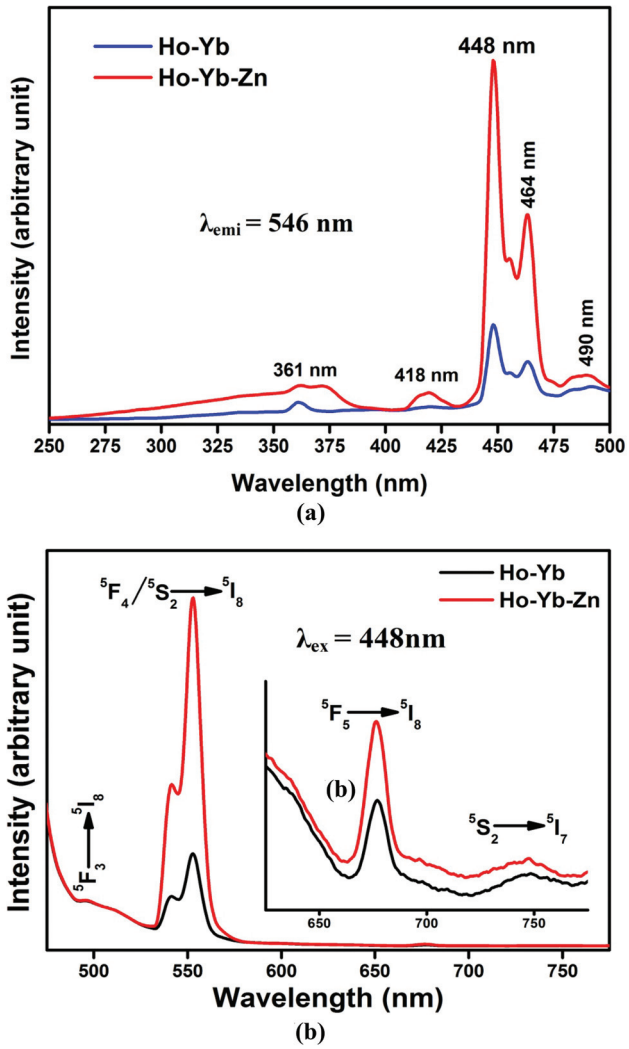

Fig. 7 (a) Excitation spectra of Y_2O_3:Ho^{3+}–Yb^{3+} and Y_2O_3:Ho^{3+}–Yb^{3+}–Zn^{2+} phosphors at 546 nm emission. (b) Photoluminescence emission spectra of Y_2O_3:Ho^{3+}–Yb^{3+} and Y_2O_3:Ho^{3+}–Yb^{3+}–Zn^{2+} phosphors at 448 nm excitation.

observed about 361 nm, 418 nm, 448 nm, 464 nm and 490 nm corresponding to the $^3H_5 \leftarrow {}^5I_8$, $^5G_5 \leftarrow {}^5I_8$, $^5G_6 \leftarrow {}^5I_8$, $^3K_8 \leftarrow {}^5I_8$ and $^5F_3 \leftarrow {}^5I_8$ transitions, respectively. The room temperature photoluminescence (PL) emission spectra of Y_2O_3:Ho^{3+}–Yb^{3+} and Y_2O_3:Ho^{3+}–Yb^{3+}–Zn^{2+} phosphors under excitation at 448 nm is shown in Fig. 7(b). It is observed that the PL emission spectra obtained upon 448 nm excitation are very similar to the UC emission spectra obtained upon 980 nm excitation except for the small shift in peak positions of all the assigned bands. The enhancement in PL intensity has also been observed in the case of Zn^{2+} codoped Y_2O_3:Ho^{3+}–Yb^{3+} matrix. It is smaller (*i.e.* about 4 times) compared to that of the UC emission (~7 times) band lying in the green region. This is again basically due to the local field effect which arises due to presence of Zn^{2+} ions in the Y_2O_3:Ho^{3+}–Yb^{3+} codoped phosphor. It is notable that the blue to green conversion of present material is very suitable for development of green light emitting diodes (LEDs) by coating on the InGaN blue chip.[5]

3.4 Temperature sensing investigation

To investigate the temperature sensing behaviour of the present phosphor material (Y_2O_3:Ho^{3+}–Yb^{3+}–Zn^{2+}), the UC emission spectra of the blue band within the 460–505 nm range upon 980 nm diode laser excitation on increasing the sample temperature from 299 to 673 K at an excitation power of nearly 250 mW have been monitored (Fig. 8). It was observed that the intensities of bands centred at 465 nm and 491 nm change very much on increasing the sample temperature but the peak position of the bands do not shift. The overall intensity of the blue band decreases on increasing the temperature of the sample due to an increase in the lattice vibrations followed by the increased non-radiative relaxation rate. The intensity of the peak at about 465 nm is much less in comparison to that at about 491 nm at room temperature (299 K), while at higher temperature (673 K) the reverse trend is observed and hence the variation in intensity ratio of two peaks has been estimated. This variation in fluorescence intensity ratio (FIR) of two close lying levels $^3K_8$ and $^5F_3$ can be written as[2,45]

$$\text{FIR } (R) = I_{465}/I_{491} = B \exp(-\Delta E/kT) \qquad \text{(iii)}$$

where I_{465} and I_{491} are the integrated intensities corresponding to the $^3K_8 \rightarrow {}^5I_8$ and $^5F_3 \rightarrow {}^5I_8$ transitions respectively, ΔE is the energy gap between the $^3K_8$ and $^5F_3$ levels, T is the absolute temperature and k is Boltzmann's constant. The pre-exponential factor B is also a constant. From eqn (iii), it is clear that the FIR is independent of the source intensity, which is an essential requirement for any temperature sensing device.

The FIR of the blue UC emission corresponding to the $^3K_8 \rightarrow {}^5I_8$ and $^5F_3 \rightarrow {}^5I_8$ transitions have been calculated at different temperatures and plotted as a function of temperature (Fig. 9). The experimental data were fitted by using eqn (iii) and matched very well with fitted curve, as is clear from Fig. 9. The value of constant B and energy gap ΔE from the fitting have been found to be 5.36 and 742.09 cm^{-1}, respectively. The fitted value of the energy gap (742.09 cm^{-1}) is

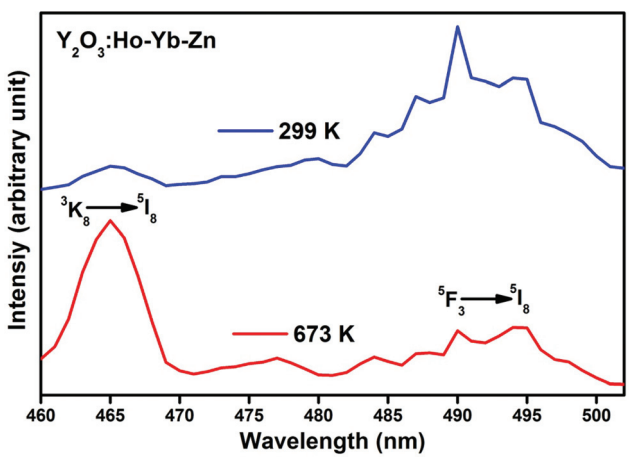

Fig. 8 Blue UC emission spectra of Y_2O_3:Ho^{3+}–Yb^{3+}–Zn^{2+} phosphor at different temperatures.

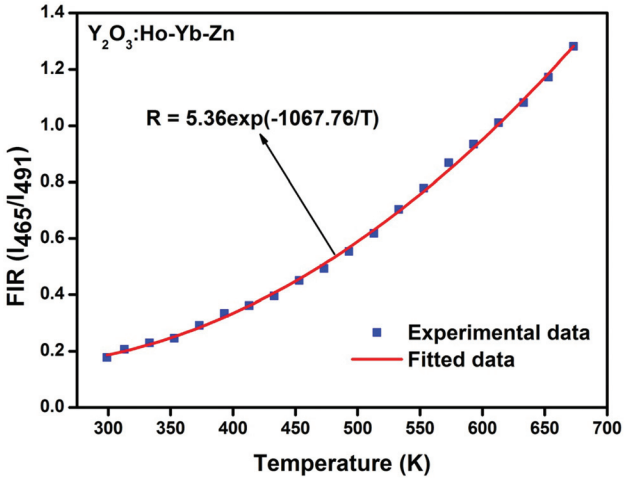

Fig. 9 Variation of FIR ($I_{465\ nm}/I_{491\ nm}$) as a function of absolute temperature.

in good agreement with actual energy gap (~750 cm^{-1}) between the two levels. Hence we can say that the $^3K_8$ and $^5F_3$ levels are thermally coupled.

Furthermore, the rate at which the FIR changes with temperature is a very important parameter to identify the applicability of the present material as an optical temperature sensor, known as sensor sensitivity[46] defined by

$$S = d(FIR)/dT = FIR \times (\Delta E/kT^2) \quad \text{(iv)}$$

where all the terms have their usual meanings as explained before. The calculated value of the sensor sensitivity as a function of temperature is presented in Fig. 10. The sensor sensitivity increases on increasing the sample's temperature, which is a good indication for the present material to be used as a temperature sensing probe. The maximum value of sensitivity is about 30.199×10^{-4} K^{-1} at 673 K temperature and seems to be improving at higher temperature.

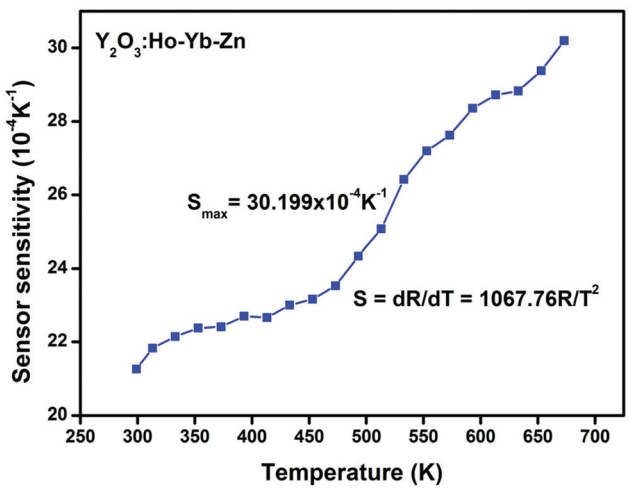

Fig. 10 Sensor sensitivity *versus* absolute temperature plot for Y_2O_3:Ho^{3+}–Yb^{3+}–Zn^{2+} phosphor.

The sensitivity of the present phosphor is good and appears to increase at higher temperatures (Fig. 10). On comparing with other reported materials,[45–51] the Y_2O_3:Ho^{3+}–Yb^{3+}–Zn^{2+} phosphor is a better material for optical sensors both in temperature range and in terms of sensor sensitivity.

4. Conclusion

In conclusion, the luminescence emission from combustion synthesized Y_2O_3:Ho^{3+}–Yb^{3+} phosphor have been enhanced by Zn^{2+} codoping upon 448 nm and 980 nm excitations and a shift was observed in 2θ value of XRD pattern due to retrenchment of the unit cell volume. The decay curve analysis shows a decrement in decay time on codoping with Zn^{2+} ions which causes an increase in the transition probability of emitting states and hence the enhancement in emission intensity. The purity of green colour emitted from sample has been improved and CIE colour coordinate was found to be much closer to the ideal value. The utilization of the present phosphor material in the development of an optical temperature sensor has been confirmed by the temperature dependent FIR study. The maximum sensitivity obtained was about 30.199×10^{-4} K^{-1} at 673 K and it seems to increase further for higher temperature. Consequently the Y_2O_3:Ho^{3+}–Yb^{3+}–Zn^{2+} codoped phosphor may be used in making an efficient green upconverter and temperature sensor with high efficiency. Also it may be used in development of green LEDs and biological applications.

Acknowledgements

Authors are grateful to the University Grants Commission, New Delhi, India for providing the financial assistance [F. No. 39-534/2010(SR)].

References

1 H. S. Marder, P. Kele, S. M. Saleh and O. S. Wolfbeis, *Curr. Opin. Chem. Biol.*, 2010, **14**, 582.
2 S. A. Wade, S. F. Collins and G. W. Baxter, *J. Appl. Phys.*, 2003, **94**, 4743.
3 R. L. Toquin and A. K. Cheetham, *Chem. Phys. Lett.*, 2006, **423**, 352.
4 T. Y. Dai, Y. L. Ju, B. Q. Yao, Y. J. Shen, W. Wang and Y. Z. Wang, *Laser Phys. Lett.*, 2012, **9**, 716.
5 S. Ye, F. Xiao, Y. X. Pan, Y. Y. Ma and Q. Y. Zhang, *Mater. Sci. Eng., R*, 2010, **71**, 1.
6 S. Fischer, J. C. Goldschmidt, P. Loper, G. H. Bauer, R. Bruggemann, K. Kramer, D. Biner, M. Hermle and S. W. Glunz, *J. Appl. Phys.*, 2010, **108**, 044912.
7 C. H. Kim, I. E. Kwon, C. H. Park, Y. J. Hwang, H. S. Bae, B. Y. Yu, C. H. Pyun and G. Y. Hong, *J. Alloys Compd.*, 2000, **311**, 33.
8 Y. Dwivedi, A. Bahadur and S. B. Rai, *J. Appl. Phys.*, 2011, **110**, 043103.

9 G. S. Maciel, R. B. Guimaraes, P. G. Barreto, I. C. S. Carvalho and N. Rakov, *Opt. Mater.*, 2009, **31**, 1735.
10 M. Rai, K. Mishra, S. K. Singh, R. K. Verma and S. B. Rai, *Spectrochim. Acta, Part A*, 2012, **97**, 825.
11 B. S. Cao, Y. Y. He, L. Zhang and B. Dong, *J. Lumin.*, 2013, **135**, 128.
12 V. Singh, V. K. Rai and M. Haase, *J. Appl. Phys.*, 2012, **112**, 063105.
13 R. Chen, Y. Wang, Y. Hu, Z. Hu and C. Liu, *J. Lumin.*, 2008, **128**, 1180.
14 V. Singh, V. K. Rai, S. Watanabe, T. K. Gundu-Rao, I. Ledoux-Rak and H. Y. Kwak, *Appl. Phys. A*, 2010, **100**, 1123.
15 S. K. Singh, K. Kumar and S. B. Rai, *Appl. Phys. B*, 2009, **94**, 165.
16 G. Liu, Y. Zhang, J. Yin and W. F. Zhang, *J. Lumin.*, 2008, **128**, 2008.
17 Y. Bai, Y. Wang, K. Yang, X. Zhang, G. Peng, Y. Song, Z. Pan and C. H. Wang, *J. Phys. Chem. C*, 2008, **112**, 12259.
18 D. W. Kim, R. Balakrishnaiah, S. S. Yi, K. D. Kim, S. H. Kim, K. Jang, H. S. Lee and J. H. Jeong, *ECS Trans.*, 2009, **16**, 13.
19 Q. Du, G. Zhou, J. Zhou, X. Jia and H. Zhou, *J. Alloys Compd.*, 2013, **552**, 152.
20 B. S. Cao, Y. Y. He, Z. Q. Feng, M. Song and B. Dong, *Opt. Commun.*, 2011, **248**, 3311.
21 H. Zhang, X. Fu, S. Niu and Q. Xin, *J. Alloys Compd.*, 2008, **459**, 103.
22 K. A. Hyeon, S. H. Byeon, J. C. Park, D. K. Kim and K. S. Suh, *Solid State Commun.*, 2000, **115**, 99.
23 M. K. Chong, K. Pita and C. H. Kam, *Appl. Phys. A*, 2004, **79**, 433.
24 R. Dey, V. K. Rai and A. Pandey, *Spectrochim. Acta, Part A*, 2012, **99**, 288.
25 S. M. Chung, S. Y. Kang, J. H. Shin, W. S. Cheong, C. S. Hwang, K. I. Cho, S. J. Lee and Y. J. Kim, *J. Cryst. Growth*, 2011, **326**, 94.
26 V. Singh, V. K. Rai, I. Ledoux-Rak, L. Badie and H. Y. Kwak, *Appl. Phys. B*, 2009, **97**, 805.
27 M. Wu, J. R. Lakowicz and C. D. Geddes, *J. Fluoresc.*, 2005, **15**, 53.
28 C. Milone, M. Trapani, R. Zanella, E. Piperopolulos and S. Galvagno, *Mater. Res. Bull.*, 2010, **45**, 1925.
29 Z. P. Li, B. Dong, Y. Y. He, B. S. Cao and Z. Q. Feng, *J. Lumin.*, 2012, **132**, 1646.
30 V. Singh, V. K. Rai, I. Ledoux-Rak and H. Y. Kwak, *Appl. Phys. B*, 2009, **97**, 103.
31 J. H. Chung, S. Y. Lee, K. B. Shim and J. H. Ryu, *Appl. Phys. Express*, 2012, **5**, 052602.
32 C. H. Yang, Y. X. Pan, Q. Y. Zhang and Z. H. Jiang, *J. Fluoresc.*, 2007, **17**, 500.
33 S. Gutzov, S. Berendts, M. Lerch, Ch. Geffert, A. Borger and K. D. Becker, *Phys. Chem. Chem. Phys.*, 2009, **11**, 636.
34 T. K. Anh, P. Benalloul, C. Barthou, L. T. K. Giang, N. Vu and L. Q. Minh, *J. Nanomater.*, 2007, 48247.
35 A. Pandey and V. K. Rai, *Appl. Phys. B*, 2012, **109**, 611.
36 A. K. Parchur and R. S. Ningthoujam, *Dalton Trans.*, 2011, **40**, 7590.
37 B. D. Cullity, *Elements of X-ray Diffraction*, Addison-Wesley, Reading, MA, 1978, vol. 1, pp. 102–110.
38 V. Singh, V. K. Rai, B. Voss, M. Haase, R. P. S. Chakradhar, D. T. Naidu and S. H. Kim, *Spectrochim. Acta, Part A*, 2013, **109**, 206.
39 A. Pandey, V. K. Rai, R. Dey and K. Kumar, *Mater. Chem. Phys.*, 2013, **139**, 483.
40 G. H. Dieke, *Spectra and Energy Levels of Rare Earth Ions in Crystals*, Interscience Publishers, USA, 1968, pp. 253–261 [SBN 470 21390 6].
41 V. K. Rai, *Appl. Phys. B*, 2010, **100**, 871.
42 J. Milliez, A. Rapaport, M. Bass, A. Cassanho and H. P. Jenssen, *J. Disp. Technol.*, 2006, **2**, 307.
43 T. Nyokong and V. Ahsen, *Photosensitizers in Medicine, Environment, and Security*, Springer Science+Business Media B. V., 2012, , DOI: 10.1007/978-90-481-3872-2.
44 M. Wang, G. Abbineni, A. Clevenger, C. Mao and S. Xu, *Nanomed. Nanotechnol.*, 2011, **7**, 710.
45 V. K. Rai, D. K. Rai and S. B. Rai, *Sens. Actuators, A*, 2006, **128**, 14.
46 W. Xu, X. Gao, L. Zheng, Z. Zhang and W. Cao, *Opt. Express*, 2012, **20**, 18127.
47 R. K. Verma and S. B. Rai, *J. Quant. Spectrosc. Radiat. Transfer*, 2012, **113**, 1594.
48 L. Liu, Y. Wang, X. Zhang, K. Yang, Y. Bai, C. Huang and Y. Song, *Opt. Commun.*, 2011, **248**, 1876.
49 C. Li, B. Dong, C. Ming and M. Lei, *Sensors*, 2007, **7**, 2652.
50 N. Rakov and G. S. Maciel, *Sens. Actuators, B*, 2012, **164**, 96.
51 C. Li, S. Li, B. Dong, Z. Liu, C. Song and Q. Yu, *Sens. Actuators, B*, 2008, **134**, 313.